IEEE Access
Multidisciplinary ⋮ Rapid Review ⋮ Open Access Journal

Received 14 February 2023, accepted 5 March 2023, date of publication 13 March 2023, date of current version 7 April 2023.

Digital Object Identifier 10.1109/ACCESS.2023.3256887

RESEARCH ARTICLE

An Optimized Carrier Phase-Shifted Modulation Strategy for Cuk PV Inverter

RENXI GONG[1,2] AND CHENG ZHAO[1]
[1]School of Electrical Engineering, Guangxi University, Nanning 530004, China
[2]School of Traffic and Transportation, Nanning University, Nanning 530200, China

Corresponding author: Renxi Gong (rxgong@gxu.edu.cn)

This work was supported in part by the National Natural Science Foundation of China under Grant 61561007; and in part by the Natural Science Foundation of Guangxi Province, China, under Grant 2017GXNSFAA198168.

ABSTRACT There exists the problems of output voltage zero-point drift and high even harmonic content of the three-phase Cuk liftable voltage photovoltaic (PV) inverter when it adopts the conventional carrier modulation method. In view of these, a new optimized Phase-Shifted Pulse Width Modulation (PSPWM) strategy is proposed. Firstly, the optimal zero-sequence component is determined based on the inverter topology and control objectives. Next, the zero-sequence component is injected into the sinusoidal signal and used as the new modulating signal so that the carrier pulse width modulation is equivalent to the space vector pulse width modulation. Finally, the carrier and modulating waveforms are blended in a superior manner, and a new logical operation is applied to generate the required switching drive signals for the control of the inverter switching tubes. In order to verify the effectiveness of the strategy, simulation and experimental platforms were constructed, and numerous simulations and experiments were done. The results show that the modulation strategy can solve the output voltage zero drift problem effectively, and suppress the even harmonics effectively, meanwhile, the harmonics are mainly concentrated near the primary frequency, which significantly reduces the total harmonic content and greatly improves the output voltage waveform. In addition, the modulation can be achieved by reducing one carrier signal, thus simplifying the modulation process and the design of the digital signal system.

INDEX TERMS Cuk PV inverter, liftable voltage inverter, PSPWM, zero-sequence component, space vector modulation.

I. INTRODUCTION

With the rapid development of photovoltaic power generation and other renewable energy generation systems, photovoltaic inverters have occupied an extremely important position in today's energy field. Along with the emergence and continuous development of various high-voltage resistant high-power devices, the traditional two-level Photovoltaic (PV) inverter can no longer meet the needs of all aspects [1]. Since the input voltage of a PV power generation system fluctuates in a wide range due to various factors such as light intensity and temperature, the inverter output needs to be flexibly adjusted to suit different situations and occasions, so multi-level PV inverters with the ability to raise and lower voltage were born [2], [3], [4], [5], [6], [7], [8], [9].

In [7], a two-stage three-phase liftable voltage three-level inverter is proposed. However, the topology increases the number of switching tubes and passive devices, leading to an increase in size and cost; and there are problems of low power transfer efficiency and complex control. In [8], a three-phase quasi-Z-source three-level inverter is proposed, but there are still problems such as large switching losses and limited boosting capacity. Aiming at these, a new single-stage three-phase Cuk liftable voltage three-level inverter was proposed, starting from the topology of the inverter itself, in [9]. The inverter features a simple structure, easy control, few passive components, high voltage gain, and high performance in both step-up and step-down, which satisfies the needs of new energy generation systems. However, this inverter suffers

The associate editor coordinating the review of this manuscript and approving it for publication was Alfeu J. Sguarezi Filho.

from output voltage zero-point drift, high even harmonic content, and limited output voltage range when conventional sinusoidal wave modulation is applied.

A new hybrid Phase-Shifted Pulse Width Modulation (PSPWM) improved synchronous optimized Pulse Width Modulation (PWM) technique was proposed in [10], which may effectively reduce the total harmonic distortion and improve the system reliability. However, this modulation strategy needs to be programmed offline to calculate the optimal switching angle of the switching tubes, which increases the complexity of the system control. A Variable Frequency Phase-Shifted PWM (VF-PSPWM) strategy was proposed in [11], which may reduce the voltage ripple and harmonic content by changing the carrier frequency according to the load current magnitude. However, it is also required to establish the quantitative relationship between the load current change and the carrier frequency change, and it may impair the fast response capability and reliability of the system. In [12] and [13], The modulation strategies based on carrier transform and modulating waveform transform were proposed, respectively, which can simplify the modulation process of the system. However, it is challenging to accomplish the capacitance-voltage balance of the flying capacitor inverter.

In [13], a unified form of Space Vector PWM (SVPWM) and carrier PWM is derived from the equation and it is proved that the bridge linking the both is the zero-sequence component. In [14], a carrier modulation strategy for the injection of zero-sequence components and midpoint potential balance control was proposed for a three-level midpoint-clamped inverter. The strategy equates carrier modulation with space vector modulation, which avoids output voltage zero-point drift and decreases output harmonic content. However, exact mathematical relationships need to be established, which is challenging to implement. Aiming at these, in [15], an optimal zero-sequence voltage injection pulse-width modulation in two-level voltage source inverter applications is proposed, and in [16], a multilevel PWM algorithm based on zero-sequence component injection for three-level rectifiers is proposed, and both literatures propose the idea of injecting optimal zero-sequence components according to different control objectives.

In view of the problems mentioned above, which have not been well solved, this paper proposes an optimal PSPWM strategy with zero-sequence component injection for the problems of the three-phase Cuk liftable voltage inverter. The optimal zero-sequence component developed in this paper are injected into the sinusoidal signal as a new modulating waveform and it is modulated with the carrier waveform in the proposed new combination. Firstly, we determine the optimal zero-sequence component to be injected based on the inverter topology and control objectives. Then, this optimal zero-sequence component is injected into the sinusoidal signal to obtain a new modulated waveform. Finally, we combine the modulating wave and carrier wave in an optimized way for carrier phase-shifted modulation and obtain the desired modulating signal with a new logic operation. The simulation platform was built to conduct relevant simulations and experiments, and the results showed that the strategy can effectively eliminates output voltage zero drift, significantly reduce harmonic content, and fully utilize the high voltage gain performance of the inverter. Meanwhile, the proposed strategy reduces one carrier signal compared to conventional carrier modulation, simplifying the modulation process and digital signal system design.

II. WORKING PRINCIPLES OF CUK LIFTABLE VOLTAGE INVERTER

A. INVERTER TOPOLOGY

The Cuk inverter studied in this paper is shown in Figure 1. The Direct Current (DC) voltage source U_{in} simulates the PV input on the DC side, $S_{\text{X1}-4}$(X = A, B and C) represent the switching tubes forming the three-phase bridge arms, and $D_{\text{A}-\text{C}}$ represent the power diodes in reverse series to prevent damage to the PV module caused by current backflow, and also includes three flying-capacitors (C_{FA}, C_{FB} and C_{FC}), an input-side inductor L_1, an intermediate energy storage capacitor C_1, and three-phase LC filter unit and load.

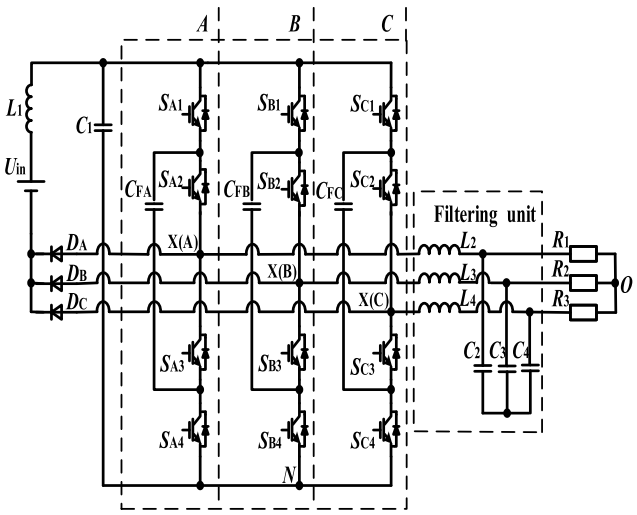

FIGURE 1. Three-phase Cuk liftable voltage inverter.

TABLE 1. Switching combinations.

Stage	S_{X1}	S_{X2}	S_{X3}	S_{X4}	u_{CF}	u_{XN}
Ⅰ	1	0	0	0	Charging	$u_{C1}/2$
Ⅱ	1	1	1	1	——	u_{C1}
Ⅲ	0	1	1	1	Discharging	$u_{C1}/2$
Ⅳ	0	0	0	0	——	0

Note: "0" means the corresponding switch is off; "1" means the corresponding switch is on; "-" means that the flying capacitor C_{FA} is neither charged nor discharged.

B. INVERTER WORKING STATUS

The three-phase inverters have the same structure in this paper. Four switching tubes S_{X1-4} in each phase are combined two by two to form the corresponding phase bridge arm, and U_{XN} represents the output level of a phase of the inverter, where "X" represents the three-phase bridge arm (X = A, B, C). There are four combinations of states in a cycle per phase as shown in Table 1.

It can be seen that in one cycle, there are three levels of "0", "$U_{C1}/2$" and "U_{C1}" for each phase output of the inverter. In the four operating states in one cycle, the flying capacitor C_{FA} is charged and discharged in switching state I and switching state III respectively, thus when the inverter adopts the carrier phase-shifted modulation method, it can make the flying capacitor charge and discharge periods equal. and the flying capacitor charging and discharging currents are equal to the sum of the input current plus the load current. So, when the inverter operates in a steady state, the flying capacitor charge and discharge currents are equal in one cycle, and the average current through the fly span capacitor is 0. Phase B and phase

C are the same as phase A. Therefore, when the inverter adopts the carrier phase-shifted modulation method, all three phases of the flying capacitor can achieve voltage self-balancing, and its steady-state voltage is equal to half of the energy storage capacitor C_1.

Taking the carrier phase-shifted modulation in phase A as an example, the ideal waveforms of each switching signal and capacitor are shown in Fig. 2.

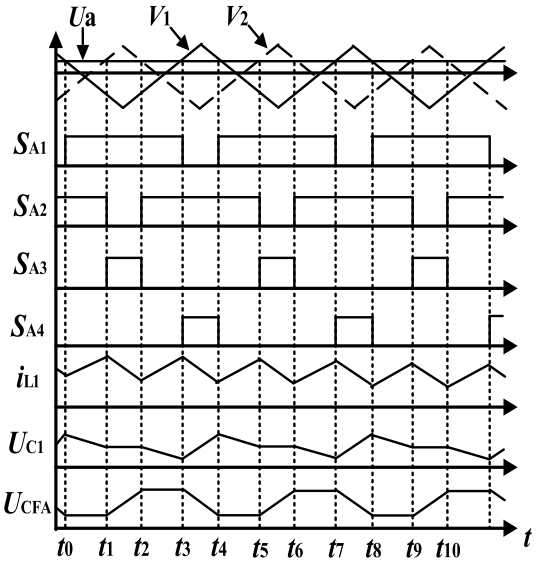

FIGURE 2. Theoretical switching signal and related waveform.

III. THE PROPOSED CARRIER PHASE-SHIFTED OPTIMIZED MODULATION STRATEGY

A. INJECTION OF ZERO-SEQUENCE COMPONENT

The double Fourier transform of the inverter in phase A is used as an example (Neglecting high-frequency carrier

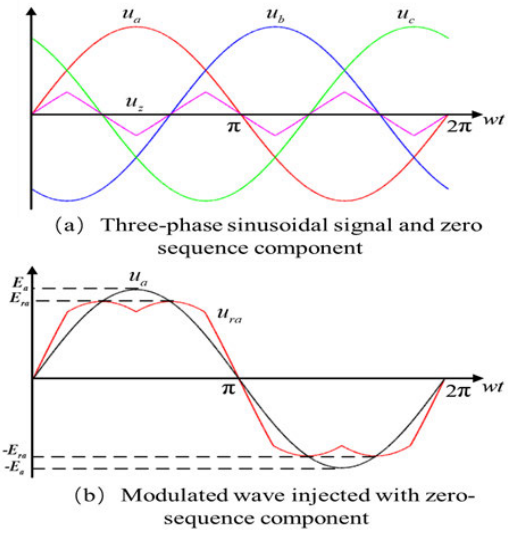

FIGURE 3. The process of injecting zero-sequence components.

harmonics and sideband harmonics of the output phase voltage). Analyzed in the case of conventional Sinusoidal Pulse Width Modulation (SPWM), the output phase voltage can be expressed as:

$$u_A = \frac{u_{C1}}{2} \cdot m \sin(\omega t) \tag{1}$$

where: ω is the fundamental angular frequency; m is the modulation ratio.

The voltage U_{C1} across the energy storage capacitor C_1 is approximated by the dc component U_{dc} and the low frequency kth harmonic component, which can be approximated as:

$$u_{C1} = [1 + \lambda \sin(k\omega t + \varphi)]\, u_{dc} \tag{2}$$

where: λ is the U_{C1} low-frequency pulsation coefficient (the ratio of the kth harmonic component to the DC component); ϕ is the initial phase of the pulsation component.

Combining (1) and (2) yields:

$$u_A = \frac{u_{dc}}{2} m \sin(\omega t) + \frac{\lambda u_{dc} m}{8} \{\cos[(k-1)\omega t + \varphi] - \cos[(k+1)\omega t + \varphi]\} \tag{3}$$

Since the upper and lower bridge arms of the inverter in this paper are asymmetric structures, when the sinusoidal signal is chosen as the modulating wave modulation, the energy storage capacitor voltage U_{C1} and the inductor current i_{L1} at the DC terminal will pulsate approximately three times the working frequency of the three-phase sinusoidal signal envelope, thus affecting the quality of the output Alternating Current (AC) voltage. So, when k =3, we can know from (3) that the output AC voltage contains second and fourth harmonic components in addition to fundamental components, resulting in zero drift of the output voltage. Therefore, this paper chooses to inject the regular sinusoidal signal with zero-sequence components as the modulating waveform.

From [17], it can be obtained that injecting the zero-sequence component into the sinusoidal modulating waveform can make the SPWM modulation method effectively equivalent to Space Vector Modulation (SVM), which not only improves the inverter DC voltage utilization and reduces the output voltage harmonic content, but also eliminates the complex vector synthesis process of space vector sinusoidal pulse width modulation. The injected zero-sequence component V_Z varies with the distribution factor k ($0 \leq k \leq 1$). In this paper, we take $k = 0.5$, from (4) and (5), we can obtain that the upper and lower parts of the modulated signal injected with zero-sequence components are symmetrical and approximate to the sinusoidal signal structure, as shown in Fig. 3.

$$\begin{cases} u_a = m \sin(wt) \\ u_b = m \sin\left(wt - \dfrac{2\pi}{3}\right) \\ u_c = m \sin\left(wt + \dfrac{2\pi}{3}\right) \end{cases} \tag{4}$$

$$\begin{cases} u_z = -\dfrac{1}{2}\left[\max\left(u_{a,b,c}\right) + \min\left(u_{a,b,c}\right)\right] \\ u_{ra,b,c} = u_{a.b.c} + u_z \end{cases} \tag{5}$$

where: the zero-sequence component U_Z is obtained from the three-phase sinusoidal reference signal U_a, U_b, and U_c; U_{ra}, U_{rb}, and U_{rc} are the three-phase modulating signal after injecting the zero-sequence component; m is the modulation ratio; ω is the modulating waveform angular frequency.

B. PROPOSED CARRIER PHASE-SHIFTED MODULATION AND OPTIMIZATION

In this paper, a carrier Phase-Shifted PWM (PSPWM) with a sinusoidal signal injected with zero-sequence components as the modulating waveform is used and optimized.

The conventional carrier phase-shifted modulation method that injects zero-sequence components into the modulating signal is shown in Fig. 4. The modulated signal U_a is compared with two triangular carriers V_1 and V_2, which are 180° phase difference, to generate the switching signals S_{X1} and S_{X2} respectively. Then the S_{X1} and S_{X2} switching signals are inverted to produce S_{X4} and S_{X3} switching signals correspondingly, and the modulation waveform is shown in Fig. 4.

In this paper, the above PSPWM modulation strategy is further optimized. Simplify two triangular carriers with 180° phase difference into one carrier signal, and then shift the modulated signal by 180° phase horizontally. We can know from analytical verification that the same delta carrier wave is compared with the modulated wave with 180° phase difference respectively, the generated switching signals have 180° phase difference and are reversed. So, the logical relationship and theoretical waveform diagram of the proposed modulation strategy are shown in Fig. 5 and Fig. 6.

It can be seen that the new modulation strategy not only reduces one carrier signal, but the modulating waveform u_{r2} can also be obtained by simply transforming the original modulating signal u_{r1}, which makes the modulation strategy easier to implement in digital signal processing systems and also gives the same inverter performance as the previous PSPWM.

Under this modulation strategy, the Cuk liftable voltage inverter studied in this paper operates in the Current

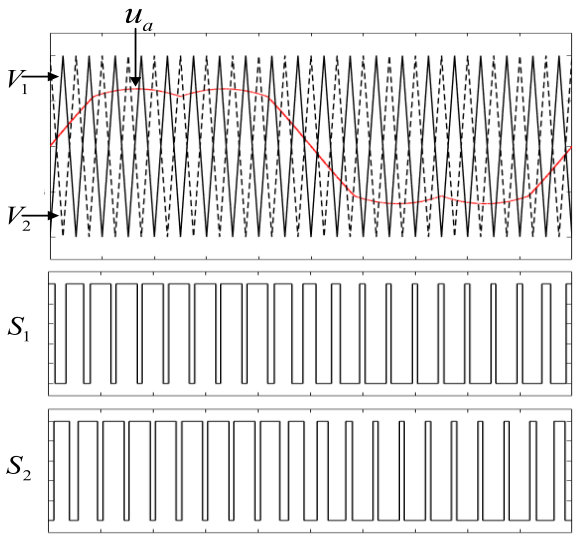

FIGURE 4. Conventional PS-PWM modulation with zero-sequence component injection.

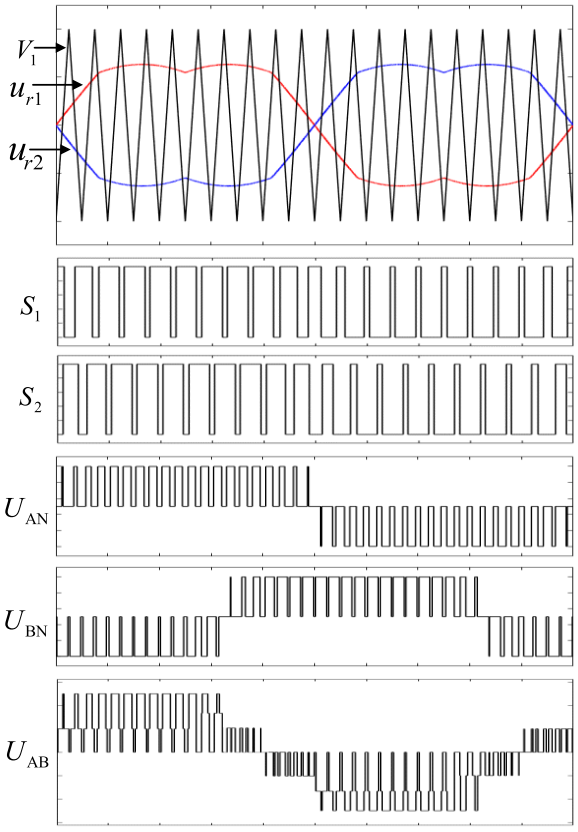

FIGURE 5. The proposed PS-PWM with zero-sequence *component.*

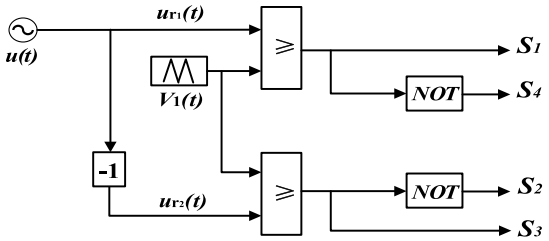

FIGURE 6. The proposed PS-PWM logic relationship.

Continuous Mode (CCM). When the inverter is operating in a steady state, assuming that the DC input is an ideal voltage source U_{in}, ignoring the harmonic components contained in the flying capacitor C_{FX} and energy storage capacitor C_1, the inverter performance is analyzed as follows:

Taking the phase A as an example, during the 1/3 cycle of the phase A modulating signal as the dominant modulating signal, the input-side inductor current i_{L1} will pulsate twice the industrial frequency, the analysis of the four operating states in each switching cycle by the volt-second balance principle is:

$$\int_{\frac{\pi}{6}}^{\frac{\pi}{2}} [\frac{U_{in}}{L_1}\left(D-\frac{1}{2}\right)T_s+\frac{U_{in}-U_{CFA}}{L_1}(1-D)\,T_s +\frac{U_{in}}{L_1}(D-2)\,T_s+\frac{U_{in}-U_{C1}+U_{CFA}}{L_1}(1-D)\,T_s]d\omega t=0 \tag{6}$$

The switching signal duty cycle D is:

$$D=\frac{1+u_{ra}}{2} \tag{7}$$

where: Ura is the phase A modulated signal after injecting the zero-sequence component. Combining (4), (5), and (7) yields:

$$D=\frac{1}{2}+\frac{m}{4}\left[\sin(\omega t)-\sin\left(\omega t-\frac{2\pi}{3}\right)\right]\left(\frac{\pi}{6}<\omega t<\frac{\pi}{2}\right) \tag{8}$$

Combining (6) and (8) yields:

$$\frac{U_{C1}}{U_{in}}=\frac{\pi m}{\pi-\frac{3\sqrt{3}}{2}m} \tag{9}$$

Because U_{C1} is equal to the inverter three-phase bridge arm bus voltage, the peak output phase voltage fundamental can be derived as:

$$U_{om}=U_{C1}\cdot\frac{m}{2}=\frac{\pi m}{\pi-\frac{3\sqrt{3}}{2}m}\cdot U_{in} \tag{10}$$

The switching tube voltage stress V_S is:

$$V_S=\frac{U_{C1}}{2}=\frac{U_{om}}{m} \tag{11}$$

Since the modulating wave is a sinusoidal signal injected with zero-sequence components, the modulation ratio m should conform to $0<m<1.154$ to avoid over-modulation

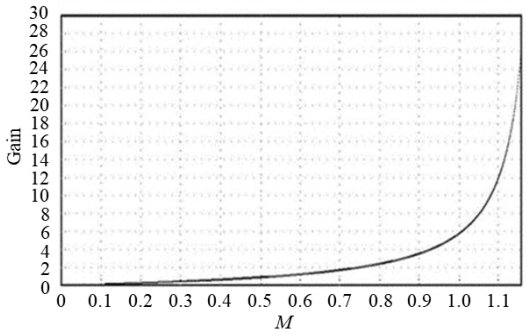

FIGURE 7. Inverter voltage gain curve.

TABLE 2. Parameters chosen in the simulation model.

parameter	value
DC supply voltage/V	100
Carrier frequency/kHz	10
Inductor L1/mH	50
Capacitor C1/uF	470
Flying capacitor C_{FX}/uF	100
Filter inductor L/mH	3
Filter capacitor C/uF	5
load	R=40Ω R=80Ω R=80Ω L=8mH

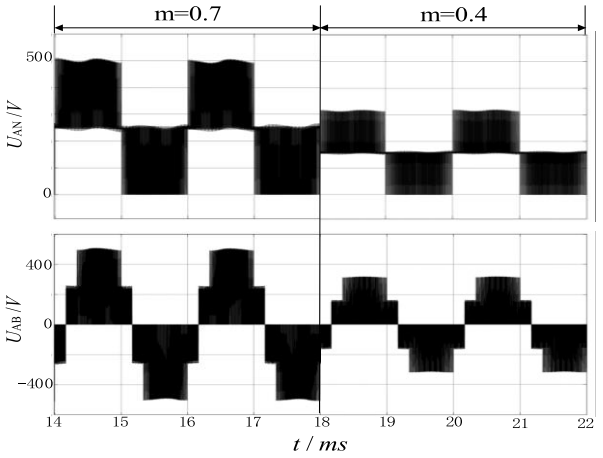

FIGURE 8. Output voltage waveform of inverter with different modulation ratios.

of the inverter. The voltage gain curve is shown in Fig. 7. we can see that the output three-phase voltage can theoretically approximate up to 25 times the input DC voltage. To ensure that the inverter operates in the linear modulation region and retains a certain safety margin, it is appropriate to control the modulation ratio m in the range of $0.3<m<1.0$. And we can deduce that when $0.547<m<1$, the inverter can achieve step-up output; when $0.3<m<0.547$, the inverter can achieve step-down output from (10).

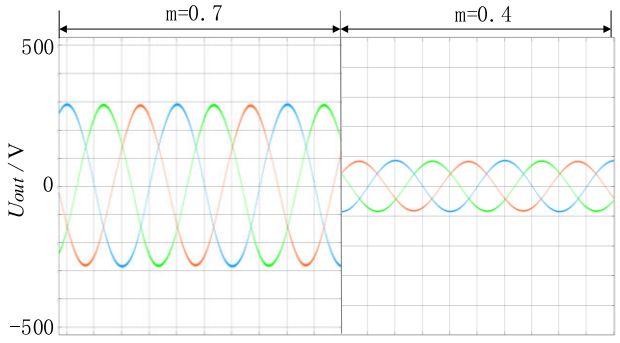

FIGURE 9. Three-phase output voltage waveforms with different modulation ratios after filtering.

TABLE 3. Comparison of different strategies and topologies.

Inverter Topology	Modulation strategy	THD of U_{AB}	Capacitor voltage self-balancing
Capacitor voltage self-balancing seven-level inverter Literature[18]	IPD-PWM	23.34%	Yes
SC-ANPC inverter Literature[19]	CO-PWM	28.72%	Yes
SI-ANPC inverter Literature[20]	3D-SVM	2.47%	No
Cuk liftable voltage inverter in the paper	SPWM	28.03%	Yes
	The proposed strategy	1.78%	

Note: U_{AB} refers to the inverter output filtered line voltage; "Yes" refers to the capacitor voltage can be self-balancing, and "No" refers to the capacitor voltage can't be self-balancing.

IV. SIMULATION ANALYSIS

In order to verify the effectiveness of the strategy proposed in this paper, MATLAB R2021a is utilized as the simulation platform to establish the Cuk liftable voltage inverter simulation model, and the circuit and modulation strategy parameters are set as shown in Table 2.

The inverter output voltage waveforms for modulation ratios $m = 0.7$ and $m = 0.4$ are shown in Fig. 8 and Fig. 9, respectively. Fig. 8 shows the output phase voltage U_{AN} of phase A and the output line voltage U_{AB} of phase A and phase B. The output voltage of U_{AN} is a three-level waveform and the output voltage of U_{AB} is a five-level waveform. Fig. 9 shows the three-phase output sinusoidal voltage waveform after filtering. It can be seen that the output waveform conforms well to the theoretical analysis, and there is no output voltage zero-point drift or waveform distortion.

Comparing the output voltage waveforms at $m = 0.7$ and $m = 0.4$, it can be seen that as the modulation ratio m decreases, the output voltage amplitude decreases significantly. In Fig. 7, the peak three-phase steady-state output voltage is about 285 V at $m = 0.7$, which is in the step-up state; the peak output phase voltage is about 84 V at $m = 0.4$, which is in the step-down state. It is verified that the inverter has the ability to raise and lower the voltage, and the step-up has a high gain.

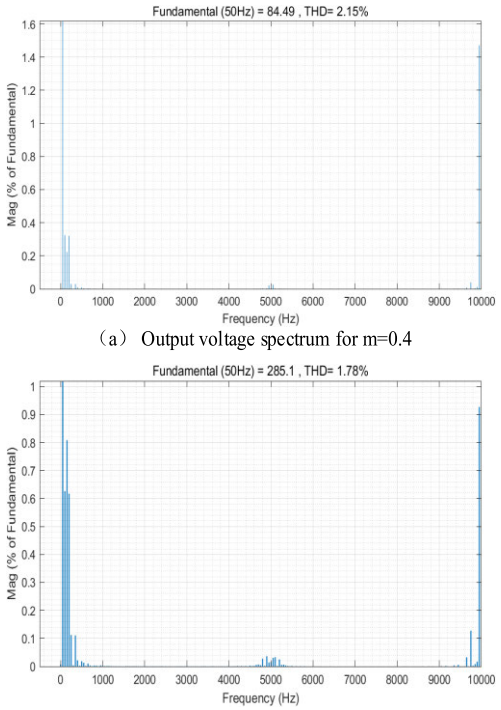

（a） Output voltage spectrum for m=0.4

（b） Output voltage spectrum for m=0.7

FIGURE 10. Frequency spectrum of output voltage with different modulation ratios.

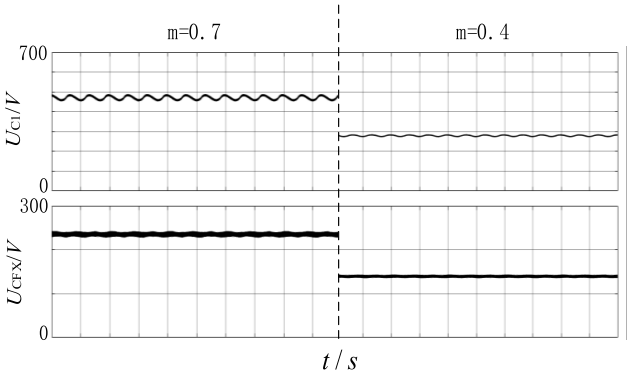

FIGURE 11. Capacitance voltage waveforms with different modulation ratios.

Fig.10 shows the output phase voltage spectrum analysis for $m = 0.4$ and $m = 0.7$. It can be seen that the fundamental amplitudes at the two modulation ratios are 84.49V and 285.1V, and the THD is 2.15% and 1.78%, respectively.

Fig. 11 shows the voltage waveforms of the energy storage capacitor C_1 and the flying capacitor C_{FX} for two modulation ratios. It can be seen from the charging and discharging process that the capacitors are able to achieve voltage self-balancing.

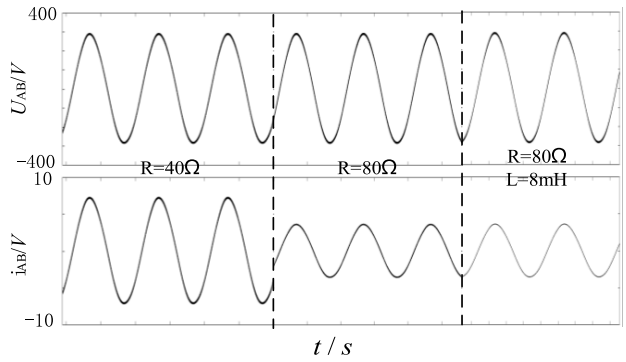

FIGURE 12. Transient response to load variations for M = 0.7.

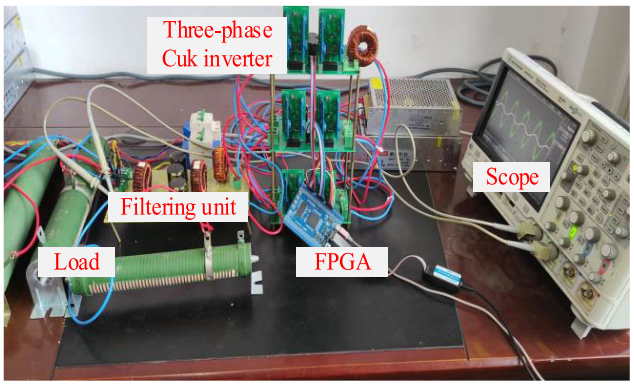

FIGURE 13. Constructed inverter experiment platform.

TABLE 4. Parameters chosen in the experimental platform.

parameter	value
DC supply voltage/V	12
Carrier frequency/kHz	10
Inductor L1/mH	50
Capacitor C1/uF	470
Flying capacitor C_{FX}/uF	100
Filter inductor L/mH	3
Filter capacitor C/uF	5
load	R=40Ω R=80Ω

Fig. 12 shows the output voltage waveforms under different load conditions for modulation ratio $m = 0.7$ and the output current change waveforms when the load changes abruptly. It can be seen that the fundamental value and THD of the output voltage hardly change for different loads, and the line current can respond quickly to changes in the load. It indicates that the inverter with the modulation strategy has strong load capability and fast response, and can maintain system stability under sudden load changes.

Table 3 shows the comparison of different strategies and different topologies. As can be seen from the table, firstly, the Cuk liftable inverter in this paper has a significant reduction in harmonic content using the proposed strategy compared

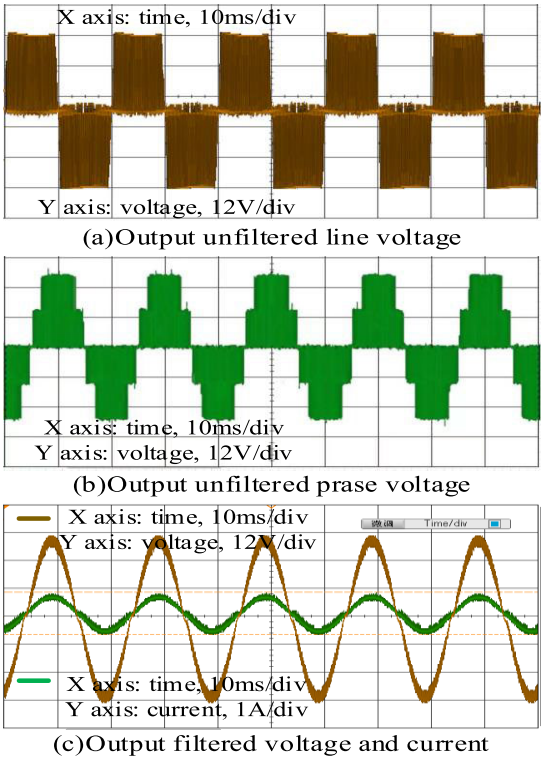

FIGURE 14. Inverter output waveform for m = 0.7.

to the conventional SPWM modulation. Furthermore, the Cuk liftable voltage inverter using the proposed modulation strategy is also superior to other different inverter topologies that can be used in PV applications. These further prove the effectiveness and superiority of the proposed modulation strategy.

V. EXPERIMENTAL VERIFICATION

To further verify the effectiveness of this modulation strategy, an experimental platform for this inverter was built, as shown in Fig. 13. The 32-channel output pulse signals are generated by the ALTERA FPGA (EP4CE6F17C8N), and the selected key parameters are shown in Table 4.

Figures 14 and 15 show the output waveforms of the inverter when the modulation ratio is 0.7 and 0.4, respectively. From their subplots (a) and (b), it can be seen that the inverter output unfiltered line voltage and phase voltage are three-level and five-level respectively, which correspond to the simulated waveform, and the voltage conforms to the theoretical step-up and step-down laws. From their subplot (c), it can be seen that the output sinusoidal voltage and current waveforms of the inverter after filtering are good, and there is no zero-point drift or waveform distortion. In addition, the peak output sinusoidal voltage at m =0.7 is about 34.2V, and the peak output sinusoidal voltage at m =0.4 is about 9V. It can be seen that although the experimental data are different from the simulation data, they match the voltage gain of the theoretical and simulation results. These also further prove

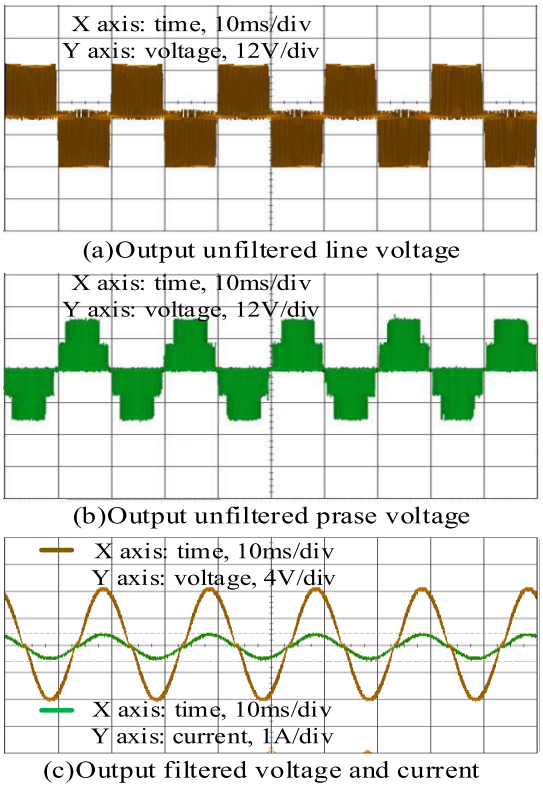

FIGURE 15. Inverter output waveform for m = 0.4.

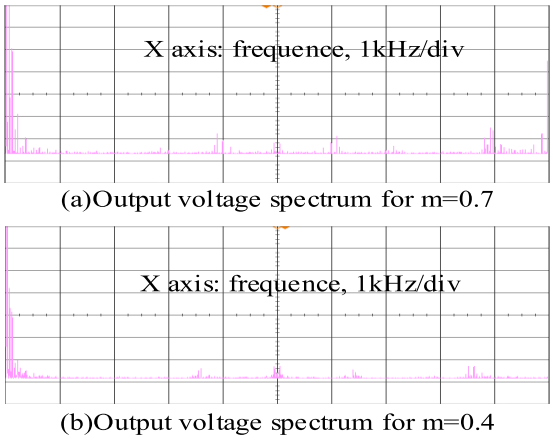

FIGURE 16. Frequency spectrum of output voltage with different modulation ratios.

the correctness and effectiveness of the strategy proposed in this paper.

Figure 16 shows the frequency spectrum of the inverter output sinusoidal voltage for $m = 0.7$ and $m = 0.4$, respectively. It can be seen that the harmonic content is significantly lower and mainly concentrated around the primary frequency, which is highly consistent with the simulation spectrum analysis results, which further verifies the effectiveness to suppress the even harmonics of the modulation strategy.

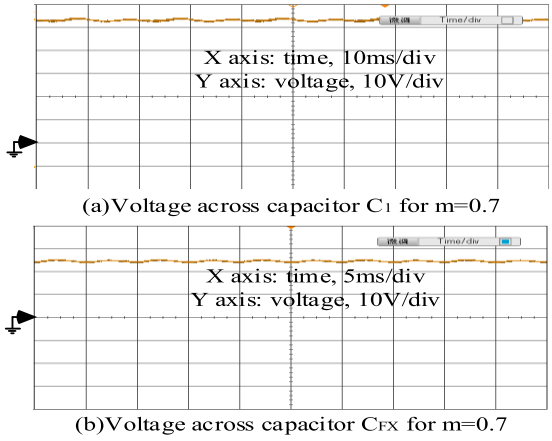

FIGURE 17. Inverter capacitor voltage waveform for m = 0.7.

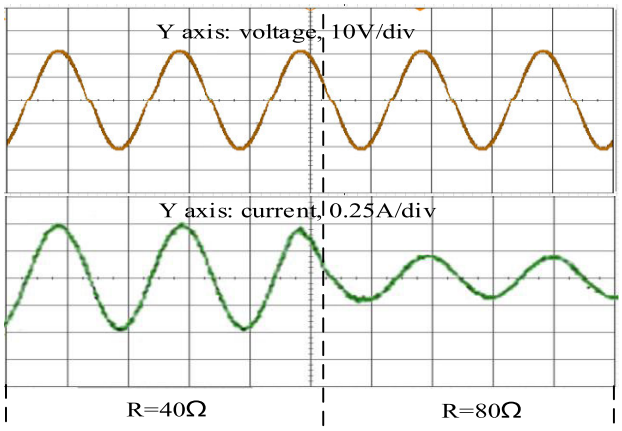

FIGURE 18. Output voltage and current waveforms with sudden load changes.

Fig. 17 illustrates the inverter capacitor voltage waveform for $m = 0.7$. From the figure, it can be seen that the capacitor voltage can achieve voltage self-balancing, which is in full agreement with the simulation results.

Figure 18 illustrates the output voltage and current waveforms measured when the inverter switches to different load conditions. It can be seen that the output voltage waveform is nearly constant when switching different loads, and the current can respond quickly to load changes. It is consistent with the simulation results and further proves that the inverter has strong load capacity and fast response capability with the modulation strategy.

VI. CONCLUSION

Aiming at the problems of zero-point voltage drift and high output voltage harmonic content in the three-phase Cuk liftable voltage inverter with conventional carrier phase-shifted modulation strategy, a new carrier phase-shifted optimized modulation strategy is proposed in this paper. A three-phase Cuk inverter simulation model and experimental platform were established, and relevant simulations and experiments were conducted. The results show that:

1) Using a sinusoidal signal injected with the optimal zero-sequence components instead of a conventional modulating signal for carrier phase-shifted modulation, can effectively eliminate the zero-point drift of the output voltage and effectively solve the problem of high harmonic content.
2) Compared to the conventional carrier phase-shifted modulation strategy, one carrier signal can be reduced, which makes the strategy easier to implement in digital signal processing systems.
3) The strategy has a large modulation ratio variation range, which can effectively exploit the step-up and step-down performance as well as the high voltage gain performance of the inverter. Well suited for photovoltaic and other renewable energy generation applications when the input voltage varies widely or the voltage level is lower.

REFERENCES

[1] L. Wang and X. Sun, *Photovoltaic Power Generation Technology in Distributed Generation Systems*, 2nd ed. Beijing, China: China Machine Press, 2014, pp. 1–7.

[2] C. M. Young and T. R. Fan, "Two-stage interleaved three-level DC/AC converter with neutral point voltage balancing," in *Proc. IFEEC ECCE Asia*, Jun. 2017, pp. 1430–1434.

[3] V. Yaramasu and B. Wu, "Predictive control of a three-level boost converter and an NPC inverter for high-power PMSG-based medium voltage wind energy conversion systems," *IEEE Trans. Power Electron.*, vol. 29, no. 10, pp. 5308–5322, Oct. 2014, doi: 10.1109/TPEL.2013.2292068.

[4] G. Yang, Y. Zhang, T. Chen, Y. Jia, and Y. Fang, "Topology and control strategy of a single-phase buck-boost five-level inverter," *Trans. China Electrotechnical Soc.*, vol. 34, no. 14, pp. 2922–2935, May 2019, doi: 10.19595/j.cnki.1000-6753.tces.l80323.

[5] L. Wang, X. Han, Z. Li, and B. Yang, "A novel flying-capacitor zeta multilevel inverter," *Trans. China Electrotech. Soc.*, vol. 37, no. 1, pp. 254–265, 2022, doi: 10.19595/j.cnki.1000-6753.tces.201222.

[6] X. Wu, J. Qi, J. Liu, A. Yang, G. Lv, Z. Zhao, and X. Zhang, "Review of multilevel inverter topology research using switched capacitor/switched inductor," *Proc. CSEE*, vol. 40, no. 1, pp. 222–233, Dec. 2019, doi: 10.13334/j.0258-8013.pcsee.190323.

[7] Z. Zhang, M Jiang, Y. Yao, and L. Kang, "Transformerless three-phase T-type three-level inverter for medium-power photovoltaic systems," in *Proc. IPEMC-ECCE Asia*, May 2016, pp. 1592–1595.

[8] O. Husev, C. Roncero-Clemente, E. Romero-Cadaval, D. Vinnikov, and T. Jalakas, "Three-level three-phase quasi-Z-source neutral-point-clamped inverter with novel modulation technique for photovoltaic application," *Electr. Power Syst. Res.*, vol. 130, pp. 10–21, Jan. 2016, doi: 10.1016/j.epsr.2015.08.018.

[9] L. Wang, X. Han, and S. Shi, "Research on a single-stage three-phase cuk three-level inverter," *Proc. CSEE*, vol. 40, no. 13, pp. 4290–4301, Feb. 2020, doi: 10.13334/j.0258-8013.pcsee.190439.

[10] B. G. Devi and B. K. Keshavan, "A novel hybrid phase shifted-modified synchronous optimal pulse width modulation based 27-level inverter for grid-connected PV system," *Energy*, vol. 178, pp. 309–317, Jul. 2019, doi: 10.1016/j.energy.2019.03.173.

[11] W. A. Khan, S. Vahid, M. R.-U. Rahman, R. Katebi, A. EL-Refaie, and N. Weise, "An optimized phase shifted PWM for flying capacitor multilevel converter," in *Proc. IEEE Energy Convers. Congr. Expo. (ECCE)*, Sep. 2019, pp. 5104–5108.

[12] S. Rahman, M. Meraj, A. Iqbal, B. P. Reddy, and I. Khan, "A combinational level-shifted and phase-shifted PWM technique for symmetrical power distribution in CHB inverters," *IEEE J. Emerg. Sel. Topics Power Electron.*, vol. 11, no. 1, pp. 932–941, Feb. 2023, doi: 10.1109/JESTPE.2021.3103610.

[13] D.-W. Chung, J.-S. Kim, and S.-K. Sul, "Unified voltage modulation technique for real-time three-phase power conversion," *IEEE Trans. Ind. Appl.*, vol. 34, no. 2, pp. 374–380, Mar. 1998, doi: 10.1109/28.663482.

[14] J. Chen, C. Wang, and J. Li, "Single-phase step-up five-level inverter with phase-shifted pulse width modulation," *J. Power Electron.*, vol. 19, no. 1, pp. 134–145, Jan. 2019, doi: 10.6113/JPE.2019.19.1.134.

[15] X. Wu, C. Li, J. Zhu, Z. Lv, X. Zhang, X. Zhang, G. Tan, and S. Xu, "An optimal zero-sequence voltage injection-based common-mode voltage reduction pulse-width modulation for the reduction of common-mode voltages in both amplitude and third-order component," *IET Power Electron.*, vol. 15, no. 14, pp. 1480–1489, May 2022, doi: 10.1049/pel2.12318.

[16] X. Yuan, Y. Li, and C. Wang, "Object oriented optimal control method for three-level PWM rectifier by zero-sequence voltage injection," *Trans. China Electrotech. Soc.*, vol. 24, no. 3, pp. 116–121, 2009.

[17] X. Chen, S. Hua, B. Li, and F. Wu, "A novel zero sequence injection scheme for three-level NPC converters considering neutral-point potential balance," *Trans. China Electrotech. Soc.*, vol. 34, no. 2, pp. 337–348,2019, doi: 10.19595/j.cnki.1000-6753.tces.171299.

[18] Z. Miao, *Research on Control Strategy of Capacitor Voltage Self-Balancing Multilevel Inverter*. Nanchang, China: East China Jiaotong Univ., May 2022.

[19] H. Yang, Z. Cheng, X. Zhang, and T. Zhou, "Multi-voltage interval modulation method and capacitor voltage control strategy for switched-capacitor Active-neutral-point-clamped multi-level converter," *Power Syst. Technol.*, pp. 1–12, Sep. 2022, doi: 10.13335/j.1000-3673.pst.2022.1208.

[20] P. Ramasamy, V. Krishnasamy, M. A. J. Sathik, Z. M. Ali, and S. H. E. A. Aleem, "Three-dimensional space vector modulation strategy for capacitor balancing in split inductor neutral-point clamped multilevel inverters," *J. Circuits, Syst. Comput.*, vol. 27, no. 14, Dec. 2018, Art. no. 1850232, doi: 10.1142/S0218126618502328.

[21] Y. Zhang, P. Huang, and Y. Bai, "A novel modulation strategy for three-level based on zero-sequence component injection," *Power Electron.*, vol. 53, no. 6, pp. 90–93, Jun. 2019.

[22] C. Wang, Y. He, Y. Liu, and J. Liu, "Research of the unity theory between the space vector and the carrier-based pulse width modulation strategies in flying capacitor multilevel inverters," *Proc. CSEE*, vol. 36, no. 15, pp. 4172–4183, Aug.2016, doi: 10.13334/j.0258-8013.pcsee.151639.

[23] D. Li and Y. Chang, "Three-level carried modulation based on zero-sequence voltage injection and control of neutral point potential," *Ind. Control Comput.*, vol. 34, no. 6, pp. 138–141, Jun. 2021.

[24] L. Xie, X. Jin, X. Wu, J. Yin, and Y. Tong, "Three-level pulse width modulation strategy based on zero-sequence voltage injection and modulation-waves decomposition," *Trans. China Electrotech. Soc.*, vol. 29, no. 10, pp. 27–37, Oct. 2014, doi: 10.19595/j.cnki.1000-6753.tces.2014.10.004.

[25] M. Ye, L. Chen, and L. Kang, "Improved carrier phase shift PWM technology based on carrier degrees of freedom," *Electr. Mach. Control*, vol. 25, no. 3, pp. 134–142, Mar. 2021, doi: 10.15938/j.emc.2021.03.015.

[26] M. Wang, X. Zhang, T. Zhao, Y. Hu, W. Mao, M. Li, and J. Xu, "An optimized third harmonic compensation strategy for single-phase cascaded H-bridge inverter," *Proc. CSEE*, vol. 40, no. 4, pp. 1073–1081, Feb. 2020, doi: 10.13334/j.0258-8013.pcsee.191140.

RENXI GONG was born in Guilin, Guangxi, China, in 1962. He received the degree in semiconductor devices and microelectronics and the Ph.D. degree in microelectronics and solid-state electronics from Xidian University, in 1993 and 2002, respectively. From 1994 to 1997, he was an Assistant Professor with Guangxi University, China, where he has been a Professor with the School of Electrical Engineering, since 2003. His current research interests include intelligent detection technology, power electronics, and their applications.

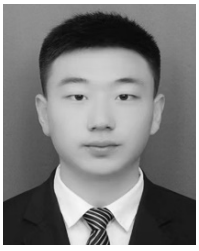

CHENG ZHAO was born in Gansu, China, in 1997. He received the B.Eng. degree from the School of Electrical Engineering and Automation, Hefei University of Technology, China. He has been majoring in electrical engineering with Guangxi University, China, since 2020. His current reserch interests include power electronics and power transmission.